Journal of Modern Optics
Vol. 00, No. 00, 00 Month 200x, 1–11

arXiv:1511.06075v1 [nlin.PS] 19 Nov 2015

Article

Semirational and symbiotic self-similar rogue waves in a (2+1)-dimensional graded-index waveguide

Kanchan Kumar De[a], Thokala Soloman Raju[b*], C. N. Kumar[c], and Prasanta K. Panigrahi[d]

[a]*Department of Physics, M.Sc. College, Saharanpur, Uttar Pradesh 247001 India*; [b]*Indian Institute of Science Education and Research (IISER) Tirupati, Andhra Pradesh 517507, India*; [c]*Department of Physics, Panjab University, Chandigarh 160014, India*; [d]*Indian Institute of Science Education and Research (IISER) Kolkata, Mohanpur, Nadia 741246, India*

(*Received 00 Month 200x; final version received 00 Month 200x*)

We have investigated the $(2+1)$-dimensional variable coefficient coupled nonlinear Schrödinger equation (vc-CNLSE) in a graded-index waveguide. Similarity transformations are used to convert the vc-CNLSE into constant coefficient CNLSE. Under certain functional constraints we could extract semirational, multi-parametric solution of the associated Manakov system. This family of solutions include known Peregrine soliton, mixture of either bright soliton and rogue wave or dark soliton and rogue wave or breather and rogue wave. Under a distinct set of self-phase modulation (SPM) and cross-phase modulation (XPM) coefficients we could establish symbiotic existence of different soliton pairs as solutions. These soliton pairs may constitute of one bright and a dark soliton, two bright solitons or two dark solitons. Finally, when two wave components are directly proportional, we find bright and dark similaritons, self-similar breathers and rogue waves as different solutions.

Keywords: Variable coefficient coupled nonlinear Schrödinger equations; Manakov system; semirational solutions; symbiotic solitons; similaritons; Akhmediev breathers; rogue waves.

1. Introduction

The mathematical model governing wave propagation in graded-index nonlinear waveguides is the variable coefficient coupled nonlinear Schrödinger equation (vc-CNLSE) [1]. Apart from this, CNLSE is one of the basic mathematical model for many physical systems. It governs the wave propagation of two overlapped wave packets in hydrodynamics [2], Langmuir and acoustic waves in plasma [3], Rossby waves [4] etc. CNLSE also describes wave propagation in twin core optical fibers [5], birefringent fibers [6] and directional couplers [7].

We shall consider $(2+1)$-dimensional vc-CNLSE in which dispersion, nonlinearity, gain and tapering function have spatial dependence. Kruglov et al. has given self-similar asymptotic solutions for equivalent $(1+1)$-dimensional equation with constant coefficients [8]. This $(1+1)$-dimensional equation in the absence of the intermodal dispersion term and with the equal strength of SPM and XPM had been investigated by Tian et al. [9] and found one- and two-soliton solutions using the Darboux method. Cardoso et al. [10] found stable solutions for a similar nonautonomous $(1+1)$-dimensional coupled NLSE. Few stable localized solutions of the two dimensional NLSE with distributed coefficients have been obtained by numerical simulations [11–13]. Recently, propagation behavior of two-breather, Kuznetsov-Ma soliton solutions were studied based on $(2+1)$-dimensional coupled NLSE [14].

In this article, we have found different semirational and symbiotic solutions for a $(2+1)$-dimensional variable coefficient coupled nonlinear Schrödinger equation (vc-CNLSE). This coupled equation is modelled for a graded-index waveguide. Similarity transformations are used to convert the coupled equations

*Corresponding author. Email: solomonr_thokala@yahoo.com

into constant co-efficient CNLSE. Under certain functional constraints we could extract semirational, multi-parametric solution of the associated Manakov system. This family of solutions include known Peregrine soliton, mixture of bright soliton and rogue wave, mixture of dark soliton and rogue wave, mixture of breather soliton and rogue wave. Also, under a distinct set of self-phase modulation (SPM) and cross-phase modulation (XPM) coefficients we could establish symbiotic existence of different soliton pairs as solutions. These soliton pairs may constitute of one bright and a dark soliton, two bright solitons or two dark solitons. Finally, for a special circumstance, when two wave components are directly proportional; we find bright and dark similaritons, self-similar breathers and rogue waves as possible solutions. Recently, some of the present authors have also studied symbiotic multimode spatial similaritons and rogons in inhomogeneously coupled optical fibers [15]. While we discuss the dynamics of these symbiotic solitons in the next sections, here we mention the seminal works done by Serkin and his group [16–18].

2. Model equation and similarity transformation

Wave propagation in inhomogeneous nonlinear waveguide can be described by the vc-CNLSE

$$i\frac{\partial u}{\partial z}+\frac{\beta(z)}{2}(\frac{\partial^2 u}{\partial x^2}+\frac{\partial^2 u}{\partial y^2})+\chi(z)(r_{11}|u|^2+r_{12}|v|^2)u+\frac{1}{2}f(z)(x^2+y^2)u=i\,g(z)u \tag{1}$$

$$i\frac{\partial v}{\partial z}+\frac{\beta(z)}{2}(\frac{\partial^2 v}{\partial x^2}+\frac{\partial^2 v}{\partial y^2})+\chi(z)(r_{21}|u|^2+r_{22}|v|^2)v+\frac{1}{2}f(z)(x^2+y^2)v=i\,g(z)v \tag{2}$$

where $u(x,y,z)$ and $v(x,y,z)$ are the the two normalized orthogonal components of electric fields. x,y are the dimensionless transverse variables and z is the dimensionless propagation distance. Here, $\beta(z),\chi(z),g(z)$ and $f(z)$ are the dispersion, nonlinearity, gain and tapering function respectively. r_{11} and r_{22} are the self-phase modulation (SPM) coefficients for $u(x,y,z)$ and $v(x,y,z)$; r_{21} and r_{12} are the cross-coupling coefficients which determine the strength of cross-phase modulation (XPM). The refractive index distribution inside the waveguide is assumed as $n=n_0+n_1f(z)(x^2+y^2)+n_2\,\chi(z)I(x,y,z)$, $I(x,y,z)$ being the optical intensity. Here, the first two terms represent the linear part of the refractive index and the last term describes a Kerr-type nonlinearity of the waveguide.

We employ gauge and similarity transformations

$$u=A(z)e^{\Omega(z)}\,\Psi_1[X(x,y,z),\zeta(z)]\exp[i\varphi(x,y,z)], \tag{3}$$

$$v=A(z)e^{\Omega(z)}\,\Psi_2[X(x,y,z),\zeta(z)]\exp[i\varphi(x,y,z)] \tag{4}$$

in Equation (1) and (2). Similarity variable and phase are assumed as

$$X(x,y,z)=\frac{kx+ly-X_c(z)}{W(z)}, \tag{5}$$

$$\varphi(x,y,z)=a(z)(x^2+y^2)+b(z)(\frac{x}{k}+\frac{y}{l})+c(z), \tag{6}$$

where $W(z)$ and $X_c(z)$ are the dimensionless beam width and position coordinate of the self-similar wave center. $a(z),b(z)$ and $c(z)$ are the parameters related to phase-front curvature, frequency shift and

phase offset respectively. When the system satisfy the following constraints

$$\Omega(z) = \int_0^z g(t)dt, \tag{7}$$

$$A(z) = \frac{A_0}{W}, \tag{8}$$

$$\chi(z) = \frac{\beta(k^2 + l^2)}{A_0^2} e^{-2\Omega(z)}, \tag{9}$$

$$f(z) = \frac{\beta W_{zz} - \beta_z W_z}{\beta^2 W}, \tag{10}$$

$$X_c(z) = 2mW \int_0^z \frac{\beta(t)}{W^2(t)} dt, \tag{11}$$

$$\zeta(z) = \int_0^z \frac{(k^2 + l^2)\beta(t)}{W^2(t)} dt, \tag{12}$$

and

$$a(z) = \frac{W_z}{2\beta W},\ b(z) = \frac{m}{W},\ c(z) = -m^2(\frac{1}{2k^2} + \frac{1}{2l^2}) \int_0^z \frac{\beta(t)}{W^2(t)} dt, \tag{13}$$

with A_0, k, l, m being real constants; Equation (1) and (2) reduces respectively to

$$i\frac{\partial \Psi_1}{\partial \zeta} + \frac{1}{2}\frac{\partial^2 \Psi_1}{\partial X^2} + (r_{11}|\Psi_1|^2 + r_{12}|\Psi_2|^2)\Psi_1 = 0 \tag{14}$$

and

$$i\frac{\partial \Psi_2}{\partial \zeta} + \frac{1}{2}\frac{\partial^2 \Psi_2}{\partial X^2} + (r_{21}|\Psi_1|^2 + r_{22}|\Psi_2|^2)\Psi_2 = 0 \tag{15}$$

In the subsequent analysis we shall assume $g(z) = \tanh z;\ A_0 = 1;\ k = l = 2;\ m = 1;\ \beta = 1; y = 0$. We also assume the form of the tapering function $f(z) = \frac{1}{\beta}(1 - 2\ \text{sech}^2 z)$ and hence, from Equation (10) we have $W(z) = \text{sech} z$.

3. Manakov system and semirational solutions

A Manakov system is the one where the values of self-phase modulation (SPM) and cross-phase modulation (XPM) are same in a coupled NLSE. Setting $r_{ij} = 1$, $(i, j = 1, 2)$ in Equation (14) and (15) we

have the associated Manakov system given by

$$i\frac{\partial\Psi_1}{\partial\zeta}+\frac{1}{2}\frac{\partial^2\Psi_1}{\partial X^2}+(|\Psi_1|^2+|\Psi_2|^2)\Psi_1=0 \tag{16}$$

and

$$i\frac{\partial\Psi_2}{\partial\zeta}+\frac{1}{2}\frac{\partial^2\Psi_2}{\partial X^2}+(|\Psi_1|^2+|\Psi_2|^2)\Psi_2=0 \tag{17}$$

This Manakov system represented by coupled Equation (16) and (17) possesses the multiparametric soliton/rogue wave solutions [19], given by

$$\begin{pmatrix}\Psi_1\\ \Psi_2\end{pmatrix}=e^{i\sigma\zeta}\left[\frac{L}{N}\begin{pmatrix}a_1\\ a_2\end{pmatrix}+\frac{M}{N}\begin{pmatrix}a_2\\ -a_1\end{pmatrix}\right], \tag{18}$$

with $L=\frac{3}{2}-2\sigma^2\zeta^2-2\sigma X^2+4i\sigma\zeta+|h|^2e^{2aX}, M=4h(aX-i\sigma\zeta-\frac{1}{2})e^{(aX+i\frac{\sigma}{2}\zeta)}$ and $N=\frac{1}{2}+2\sigma^2\zeta^2+2\sigma X^2+|h|^2e^{2aX}$. Here, a_1 and a_2 are arbitrary real parameters. Actually, a_1 and a_2 are the amplitudes of the background plane waves. h is a complex arbitrary constant and $\sigma=a^2=a_1^2+a_2^2$. These solutions have both exponential and rational dependence on coordinates and, therefore, they are called semirational. For special parameter values, these solutions produce known rogue waves such as the Peregrine soliton, mixture of bright soliton and rogue wave or mixture of dark soliton and rogue wave.
The corresponding expressions of intensity can be written as

$$\begin{pmatrix}I_u\\ I_v\end{pmatrix}=\frac{A_0^2e^{2\Omega}}{W^2}\left[\frac{|L|^2}{|N|^2}\begin{pmatrix}a_1^2\\ a_2^2\end{pmatrix}+\frac{2Re(LM^*)}{|N|^2}\begin{pmatrix}a_1a_2\\ -a_1a_2\end{pmatrix}+\frac{|M|^2}{|N|^2}\begin{pmatrix}a_2^2\\ a_1^2\end{pmatrix}\right]. \tag{19}$$

Setting $h=0$ implies $M=0$; in this particular case the expression (18) yields the rational Peregrine

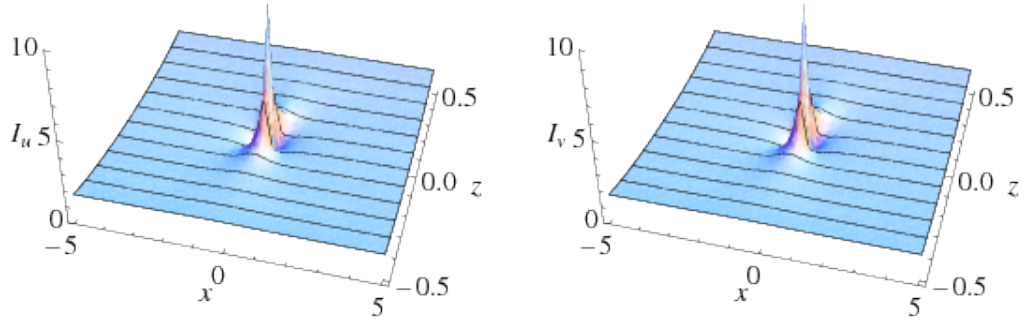

Figure 1. Freak waves intensity patterns I_u and I_v of Equation (19). Here, $a_1=1, a_2=1, h=0$.

solution [20, 21]. In this case Ψ_1 is merely proportional to Ψ_2. In Figure 1 we note that the intensity is peaked at $x=0$ and $z=0$ with the maximum value $9a_j$.
Each wave component Ψ_j is generically a mixture of a dark and a bright pulse. The superposition of the dark and bright contributions in each of the two wave components may give rise to complicated pulses. For small values of $|h|$, Peregrine and dark/bright solitons coexists separately as shown in Figure 2. By

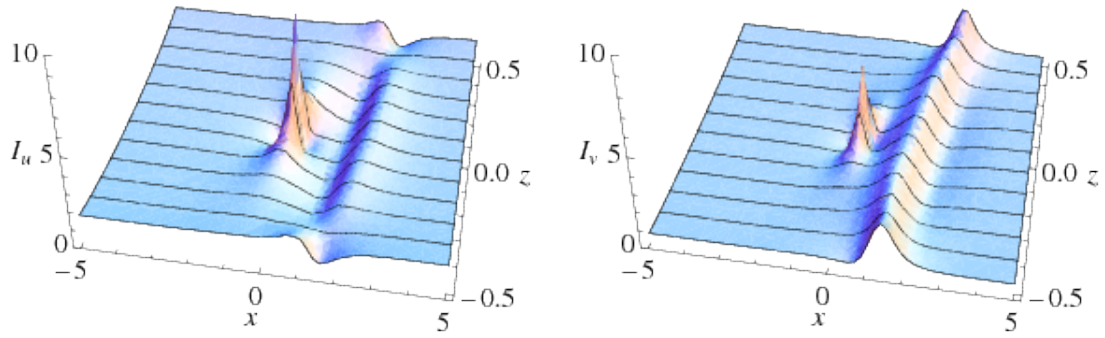

Figure 2. Intensity patterns I_u and I_v for $a_1 = 1, a_2 = 0.6, h = 0.1$.

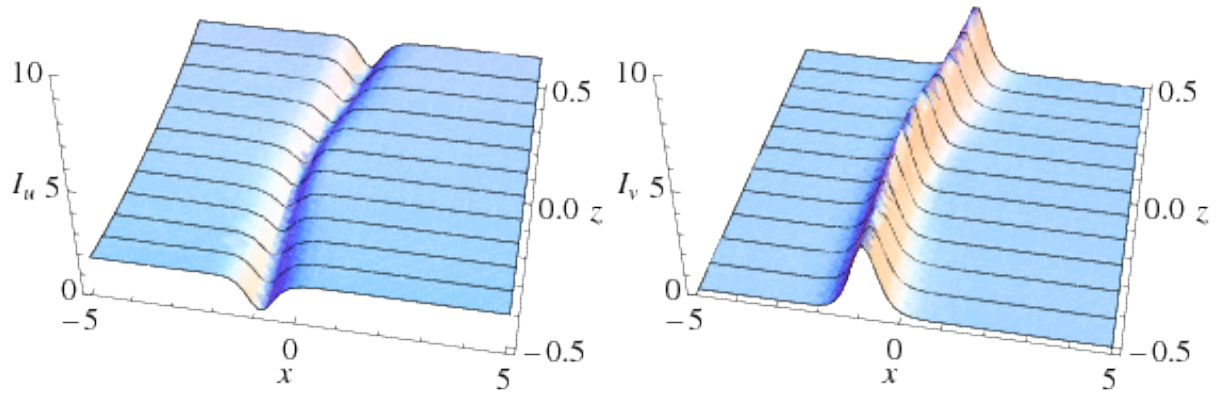

Figure 3. Intensity patterns I_u and I_v for $a_1 = 1, a_2 = 0, h = 15$.

increasing $|h|$, Peregrine and dark/bright solitons merge as shown in Figure 3. In this case, Peregrine bump cannot be identified and the resulting bright/dark pulse appear as a boomeron-type soliton, i.e., a soliton solution with time dependent velocity [22, 23]. In general one can infer that, if $h \neq 0$ the Peregrine bump coexists with bright and dark solitons.

If all parameters h, a_1, a_2 are nonvanishing, Equation (18) describes the dynamics of a breather-like wave along with Peregrine soliton. Again, for small values of $|h|$ Peregrine and breather-like soliton coexists separately as shown in Figure 4. For increased $|h|$ value, Peregrine and breather soliton merge, as shown in Figure 5.

3.1. *Generalized tapering and freak wave intensity*

We shall now discuss the effects of tapering on the intensity of the freak waves represented by Equation (19). Based on the results of supersymmetric quantum mechanics, we generate a class of tapering

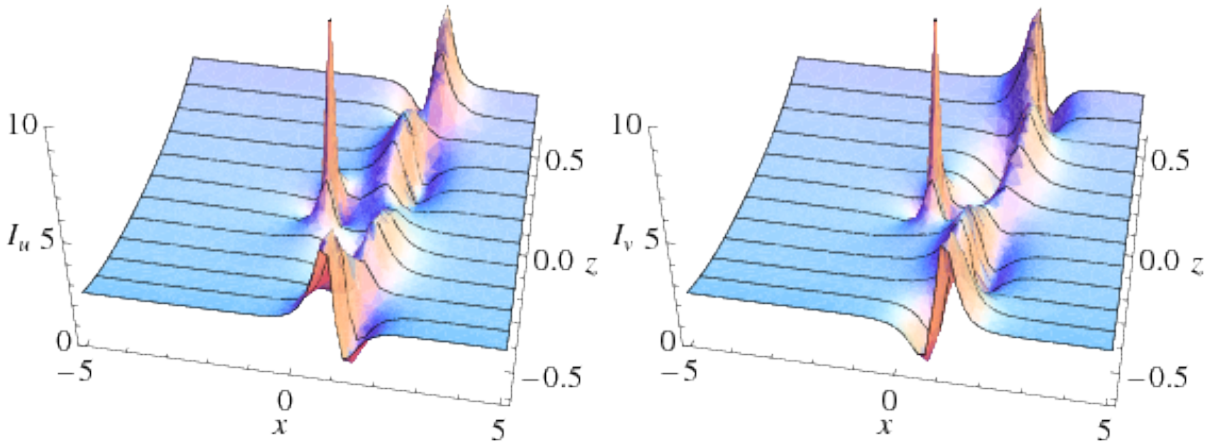

Figure 4. Intensity patterns I_u and I_v for $a_1 = 1.1, a_2 = 1.1, h = \frac{i}{15}$.

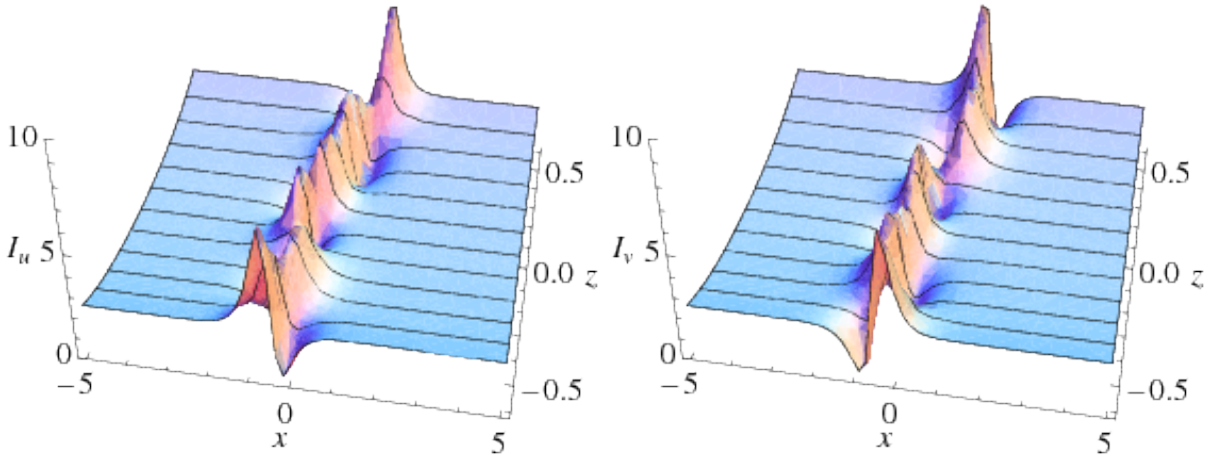

Figure 5. Intensity patterns I_u and I_v for $a_1 = 1.1, a_2 = 1.1, h = 15i$.

function and width as [24, 25]

$$\widehat{f}(z) = f(z) - \frac{2}{\beta}\frac{d}{dz}\left(\frac{W^2(z)}{c + \int_{-\infty}^{Z} W^2(s)ds}\right), \tag{20}$$

$$\widehat{W}(z) = \frac{\sqrt{c(c+1)}\, W(z)}{c + \int_{-\infty}^{Z} W^2(s)ds}, \tag{21}$$

where c is an integration constant, known as Riccati parameter and $c \notin [-2, 0]$. $\widehat{f}(z)$ is called generalized tapering function and $\widehat{W}(z)$, the generalized width. We shall consider sech^2-type tapering commonly

used in fiber optics. As described in section II a compatible pair of tapering function and width are

$$f(z) = \frac{1}{\beta}[1 - 2\ \text{sech}^2 z] \text{ and } W(z) = \text{sech}\ z. \tag{22}$$

It is now straight forward to obtain a class of $\widehat{f}(z)$ and $\widehat{W}(z)$ from Equation (20) and (21) as

$$\widehat{f}(z) = f(z) - \frac{2}{\beta}\frac{d}{dz}\left(\frac{\text{sech}^2 z}{c + (1 + \tanh z)}\right) \tag{23}$$

and

$$\widehat{W}(z) = \frac{\sqrt{c(c+1)}\,\text{sechz}}{c + (1 + \tanh z)}. \tag{24}$$

Figure 6 depicts the intensity variation with generalized width. We observe that, decrease in Riccati parameter value results in increase of intensity. Another important observation is that, the distance between the Peregrine soliton and dark/bright solitons increases with the increasing value of Riccati parameter.

4. Symbiotic similaritons

Equation (14) and (15) may possess different soliton pairs as solutions. These soliton pairs may appropriately be called as the symbiotic solitons; because each wave in the pair depends crucially on the cross-phase modulation from the complementary wave [26, 27]. In general, both solitons are interdependent on each other.
Assuming $\Psi_1 = p\ e^{i\rho\zeta}\ \text{sech}[\eta X]$ and $\Psi_2 = q\ e^{i\omega\zeta}\tanh[\eta X]$ as the general form of the bright-dark soliton solutions of Equation (14) and (15); we have [28]

$$\Psi_1 = p\ e^{i\frac{(r_{11}r_{22}-2r_{11}r_{12}+r_{12}r_{21})}{2(r_{22}-r_{12})}p^2\zeta}\ \text{sech}\left[\sqrt{\frac{(r_{11}r_{22}-r_{12}r_{21})}{(r_{22}-r_{12})}}\,pX\right] \tag{25}$$

and

$$\Psi_2 = p\sqrt{\frac{r_{21}-r_{11}}{r_{22}-r_{12}}}\ e^{i\frac{r_{22}(r_{21}-r_{11})}{(r_{22}-r_{12})}p^2\zeta}\ \tanh\left[\sqrt{\frac{(r_{11}r_{22}-r_{12}r_{21})}{(r_{22}-r_{12})}}\,pX\right], \tag{26}$$

where p is any arbitrary real constant. The expressions for intensity of the bright-dark similariton solutions can be written as

$$I_{u_B}(x,y,z) = \frac{A_0^2}{W^2}p^2e^{2\Omega}\ \text{sech}^2\left[\sqrt{\frac{(r_{11}r_{22}-r_{12}r_{21})}{(r_{22}-r_{12})}}\,pX\right], \tag{27}$$

$$I_{v_D}(x,y,z) = \frac{A_0^2}{W^2}p^2e^{2\Omega}\frac{(r_{21}-r_{11})}{(r_{22}-r_{12})}\ \tanh^2\left[\sqrt{\frac{(r_{11}r_{22}-r_{12}r_{21})}{(r_{22}-r_{12})}}\,pX\right]. \tag{28}$$

In Figure 7 we have plotted intensity of bright-dark soliton pair, corresponding to Equation (27) and (28) for a set of values for coupling coefficients and parameter p. Similarly, we have bright-bright soliton

solutions

$$\Psi_1 = p\, e^{i\frac{(r_{11}r_{22}-r_{12}r_{21})}{2(r_{22}-r_{12})}p^2\zeta}\ \text{sech}\left[\sqrt{\frac{(r_{11}r_{22}-r_{12}r_{21})}{(r_{22}-r_{12})}}\, pX\right], \tag{29}$$

$$\Psi_2 = p\sqrt{\frac{r_{11}-r_{21}}{r_{22}-r_{12}}}\, e^{i\frac{(r_{11}r_{22}-r_{12}r_{21})}{2(r_{22}-r_{12})}p^2\zeta}\ \text{sech}\left[\sqrt{\frac{(r_{11}r_{22}-r_{12}r_{21})}{(r_{22}-r_{12})}}\, pX\right] \tag{30}$$

and dark-dark soliton solutions

$$\Psi_1 = p\, e^{i\frac{(r_{11}r_{22}-r_{12}r_{21})}{(r_{22}-r_{12})}p^2\zeta}\ \tanh\left[\sqrt{\frac{(r_{12}r_{21}-r_{11}r_{22})}{(r_{22}-r_{12})}}\, pX\right], \tag{31}$$

$$\Psi_2 = p\sqrt{\frac{r_{11}-r_{21}}{r_{22}-r_{12}}}\, e^{i\frac{(r_{11}r_{22}-r_{12}r_{21})}{(r_{22}-r_{12})}p^2\zeta}\ \tanh\left[\sqrt{\frac{(r_{12}r_{21}-r_{11}r_{22})}{(r_{22}-r_{12})}}\, pX\right]. \tag{32}$$

Such types of solution pairs have been observed experimentally in photo-refractive materials [29] and also in the multi-component BEC in the harmonic trap [30]. Observing these solution pairs it is clear that, the amplitude and phase of the propagating wave components can be controlled by varying the strength of the SPM and XPM coefficients. Also, due to different feasibility conditions, these solution pairs cannot exist simultaneously.

Finally, we shall discuss about a special case where the two wave components are directly proportional to each other.

4.1. *Proportional similaritons, breathers and rogons*

For $\Psi_2 = \sqrt{\frac{r_{21}-r_{11}}{r_{12}-r_{22}}}\,\Psi_1$ and $\Psi_1 \equiv \Psi$ both Equation (14) and (15) reduces to

$$i\frac{\partial\Psi}{\partial\zeta} + \frac{1}{2}\frac{\partial^2\Psi}{\partial X^2} + \kappa|\Psi|^2\Psi = 0 \tag{33}$$

where $\kappa = \frac{r_{12}r_{21}-r_{11}r_{22}}{r_{12}-r_{22}}$.
Now, assuming the general form of the bright soliton as $\text{sech}[p(X-v\zeta)]\exp[iq(X-\omega\zeta)]$; we have

$$\Psi_B = \text{sech}[\sqrt{\kappa}(X-v\zeta)]\, e^{iv(X-\frac{v^2-\kappa}{2v}\zeta)}, \tag{34}$$

the bright soliton solution of Equation (33) where v is the velocity of the bright soliton.
Similarly, assuming the general form of the fundamental dark soliton as $(q\tanh[q(X-v\zeta)] + i\,p)\exp(i\omega\zeta)$; we have for $\kappa = -1$ i.e. for $r_{12}(r_{21}+1) = r_{22}(r_{11}+1)$,

$$\Psi_D = [q\tanh[q(X-v\zeta)] + i\,v]\, e^{-i(v^2+q^2)\zeta}, \tag{35}$$

the dark soliton solution of Equation (33). Here v is the velocity of dark soliton and q is an arbitrary real constant.

For the focussing nonlinearity, Equation (33) has another localized solution called Akhmediev breathers given by

$$\Psi_{AB} = \frac{1}{\sqrt{\kappa}} \frac{\cos(\sqrt{2}X) + i\sqrt{2}\sinh\zeta}{\cos(\sqrt{2}X) - \sqrt{2}\cosh\zeta} e^{i\zeta} \tag{36}$$

The breathers are nonlinear waves which can carry energy in a localized and oscillatory fashion. In contrast to solitons which are localized in X, the breathers are localized in ζ and oscillating in X. The breathers are not only a mathematical concept but they have also been realized experimentally in different systems such as in BEC [31], dispersion managed optical waveguides and fibers [32] and Josephson arrays [33]. Breather solutions have been obtained for various nonlinear evolution equations like KdV [34], Gardener equation [35], modified-KdV [36] and NLSE. In the context of NLSE, these spatially periodic solutions are termed as Akhmediev breathers.
Equation (33) has rogue wave solution with the following basic structure:

$$\Psi_{R_\nu} = \frac{1}{\sqrt{\kappa}} \left[(-1)^\nu + \frac{H_\nu(X,\zeta) + iK_\nu(X,\zeta))}{D_\nu(X,\zeta)} \right] e^{i\zeta}, \tag{37}$$

where ν is the order of the solution; H_ν, K_ν, D_ν are polynomials of different order. For first order rogue wave solution

$$H_1 = 4, \tag{38}$$

$$K_1 = 8\zeta, \tag{39}$$

$$D_1 = 1 + 4\zeta^2 + 4X^2. \tag{40}$$

The 2nd order rogue wave solution is the $\nu = 2$ version of Equation (37), with

$$H_2 = 12[3 - 16X^4 - 24X^2(4\zeta^2 + 1) - 4\alpha X - 80\zeta^4 - 72\zeta^2 + 4\gamma\zeta], \tag{41}$$

$$K_2 = 24[\zeta(15 - 16X^4 + 24X^2 - 4\alpha X) - 8(4X^2 + 1)\zeta^3 - 16\zeta^5 + \gamma(2\zeta^2 - 2X^2 - \frac{1}{2})], \tag{42}$$

and

$$\begin{aligned} D_2 = {} & 64X^6 + 48X^4(4\zeta^2 + 1) + 12X^2(3 - 4\zeta^2)^2 + 64\zeta^6 + 432\zeta^4 + 396\zeta^2 + 9 \\ & + \alpha[\alpha + 4X(12\zeta^2 - 4X^2 + 3)] + \gamma[\gamma + 4\zeta(12X^2 - 4\zeta^2 - 9)], \end{aligned} \tag{43}$$

where α and γ are arbitrary real constants. Rogue wave, sometimes known as freak wave or monster wave is briefly formed, single, exceptionally large amplitude wave. Rogue waves are localized both in X and ζ. These waves are of great interest in a variety of complex systems, from optics and fluid dynamics to Bose-Einstein condensates and finance. We should mention here that, just as solitary waves are known as solitons, the term rogons is coined for rogue waves. The corresponding terminologies 'oceanic rogons', 'optical rogons' and 'matter rogons' are used in the field of hydrodynamics, nonlinear optics and BECs, respectively.
Now, $I_v = aI_u$ where $a = \frac{r_{21} - r_{11}}{r_{12} - r_{22}}$. Because of the constant scaling factor the intensity I_v will have same profile as I_u for $a > 0$. Therefore, in this section we shall draw intensity diagrams associated to I_u only.

The general expression of the intensity for bright similaritons I_B, self-similar Akhmediev breathers I_{AB}, self-similar first-order rogue waves I_{R_1} and self-similar second-order rogue waves I_{R_2} are given as

$$I_B(x,y,z) = \frac{A_0^2 e^{2\Omega}}{W^2}\text{sech}^2[\sqrt{\kappa}(X - v\zeta)], \tag{44}$$

$$I_{AB}(x,y,z) = \frac{A_0^2 e^{2\Omega}}{\kappa W^2}\left[\frac{\cos^2(\sqrt{2}X) + 2\ \sinh^2\zeta}{\left(\cos(\sqrt{2}X) - \sqrt{2}\cosh\zeta\right)^2}\right], \tag{45}$$

$$I_{R_1}(x,y,z) = \frac{A_0^2 e^{2\Omega}}{\kappa W^2}\left[1 + 8\frac{1 + 4\zeta^2 - 4X^2}{(1 + 4\zeta^2 + 4X^2)^2}\right], \tag{46}$$

$$I_{R_2}(x,y,z) = \frac{A_0^2 e^{2\Omega}}{\kappa W^2}\left[\frac{K_2^2 + (H_2 + D_2)^2}{D_2^2}\right]. \tag{47}$$

In Figure 8 we have shown intensity profiles of self-similar bright soliton, Akhmediev breather, first-order rogue wave and second-order rogue wave corresponding to Equation (44)-(47), respectively, for a fixed set values for coupling coefficients and velocity.

For $\kappa = -1$, we have dark soliton solution represented by Equation (35). Hence, the general expression of the intensity for dark similaritons I_D is

$$I_D(x,y,z) = \frac{A_0^2 e^{2\Omega}}{W^2}(v^2 + q^2\tanh^2[q(X - v\zeta)]). \tag{48}$$

In Figure 9 we have plotted intensity of self-similar dark soliton, corresponding to Equation (48) for particular values of parameters v and q.

5. Conclusion

We have used similarity transformations to convert vc-CNLSE into constant co-efficient CNLSE. For the associated Manakov system, we could extract a novel multi-parametric solution having both exponential and rational dependence on coordinates, under certain functional constraints. This novel solution generate a family of solutions for different parameter values; e.g. Peregrine soliton (rational), combination of either bright soliton and rogue wave or dark soliton and rogue wave or breather soliton and rogue wave. We have also shown the effect of generalized tappering on the intensity of these semirational waves by changing Riccati parameter. Further, we could establish symbiotic existence of different soliton pairs as solutions for a set of self-phase modulation (SPM) and cross-phase modulation (XPM) coefficients. These solution pairs may consists of one bright and one dark soliton, two bright solitons or two dark solitons. Finally, assuming direct proportionality between wave components, we could extract bright and dark similaritons, self-similar breathers and rogue waves as solutions. Because of the universality of the vc-CNLSE, these solutions may contribute to better control and understanding of various solitary wave phenomena in a variety of complex dynamics, ranging from fluid dynamics, to optical communications, Bose-Einstein condensates, and financial systems.

For future studies, one can investigate the effect of gain on nonlinearity and the wave intensity. Studies regarding stability of the different solution is also an open problem.

Acknowledgement

T.S.R. acknowledges support from the DST, Government of India, through Fast Track Project Ref. No.–SR/FTP/PS-132/2012, during the course of this work.

References

[1] Agrawal, G.P. *Nonlinear Fiber Optics*, Academic Press; 2007.
[2] Dhar, A.K.; Das, K.P. *Phys. of Fluids A* **1991**,3,3021-3026.
[3] Som, B.K.; Gupta, M.R.; Dasgupta, B. *Phys. Lett. A* **1979**,72, 111-114.
[4] Sun, J.Q.; Ma, Z.Q.; Qin, M.Z. *Appl. Math. Comput.* **2006**, 183, 946-952.
[5] Huanag, D.; Li, H. *Int. J. Infrared Millimeter Waves* **2001**, 22, 93-100.
[6] Menyuk, C.R.J. *Opt. Soc. Am. B* **1988**,5, 392-402.
[7] Boumaza, N.; Benouaz, T.; Chikhaoui, A.; Cheknane, A. *Int. J. Phys. Sci.* **2009**, 4, 505513.
[8] Kruglov, V.I; D. Mechin, D.; J.D. Harvey, J.D. *Phys. Rev. A* **2008**, 77, 033846.
[9] Tian, J.; Li, J.; Kang, L.; Zhou, G. *Phys. Scr.* **2005**, 72, 394-398.
[10] Cardoso, W.B.; Avelar, A.T.; Bazeia, D. *Phys. Rev. E* **2012**, 86, 027601.
[11] Alexandrescu, A.; Montesinos, G.D.; Pérez-García, V.M. *Phys. Rev. E* **2007**, 75, 046609.
[12] Xu, S.L.; Petrović, N.Z.; Belić, M.R. *Phys. Scr.* **2013**, 87, 045401.
[13] Dai, C.Q.; Zhu, S.Q; Wang, L.L.; Zhang, J.F. *Europhys. Lett.* **2010**, 92, 24005.
[14] Dai, C.Q; Zhu, H.P. *J. Opt. Soc. Am. B* **2013**, 30, 3291-3297.
[15] Gupta, R.; Goyal, A.; Raju, T.S.; Kumar, C.N.*J.Mod. Opt.* **2013**, 60, 1569-1575.
[16] Serkin, V.N.; Hasegawa, A. and Belyaeva, T.L. *Phys. Rev. Lett.* **2007**, *98*, 074102.
[17] Serkin, V.N.; Hasegawa, A. and Belyaeva, T.L. *J. Mod. Opt.* **2010**, *57*, 1456.
[18] Serkin, V.N.; Hasegawa, A. and Belyaeva, T.L. *Phys. Rev. A* **2010**, *81*, 023610.
[19] Baronio, F.; Degasperis, A.; Conforti, M.; Wabnitz, S. *Phys. Rev. Lett.* **2012**, 109, 044102.
[20] Peregrine, D.H. *J. Aust. Math. Soc.* **1983**, 25, 16-43.
[21] Bludov, Y.V.; Konotop, V.V.; Akhmediev, N. *Eur. Phys. J. - Special Topics* **2010**, 185, 169.
[22] Degasperis, A.; Conforti, M.; Baronio, F.; Wabnitz, S. *Phys. Rev. Lett.* **2006**, 97, 093901.
[23] Conforti, M.; Baronio, F.; Degasperis, A.; Wabnitz, S. *Phys. Rev. E* **2006**, 74, 065602.
[24] Kumar, C.N.; Gupta, R.; Goyal, A.; Loomba, S.; Raju, T.S.; Panigrahi, P.K. *Phys. Rev. A* **2012**, 86, 025802.
[25] Goyal, A.; Gupta, R.; Kumar, C.N.; Raju, T.S.; Panigrahi, P.K. *Opt. Comm.* **2013**, 300, 236-243.
[26] Lisak, M.; Höök, A.; Anderson, D. *J. Opt. Soc. Am. B* **1990**,7, 810-814.
[27] Kivsher, Y.S.; Anderson, D.; Höök, A.; Lisak, M.; Afanasjev, A.A.; Serkin, V.N. *Phys. Scr.* **1991**, 44, 195-202.
[28] Ablowitz, M.J. *Nonlinear Dispersive Waves: Asymptotic Analysis and Solitons*, Cambridge University Press; 2011.
[29] Christodoulides, D.N.; Singh, S.R.; Carvalho, M.I.; Segev,M. *Appl. Phys. Lett.* **1996**, 68, 1763-1765.
[30] Yan, D.; Chang, J.J.; Hamner, C.; Kevrekidis, P.G.; Engels, P.; Achilleos, V.; Frantzeskakis, D.J.; Carretero-Gonzlez, R.; Schmelcher, P. *Phys. Rev. A* **2011**, 84, 053630.
[31] Trombettoni, A.; Smerzi, A. *Phy. Rev. Lett.* **2001**,86, 2353.
[32] Kutz, J.N.; Evangelides, S.G. *Opt. Lett.* **1998**, 23, 685-687.
[33] Trias, E.; Mazo, J.J.; Orlando, T.P. *Phys. Rev. Lett.* **2000**, 84, 741.
[34] Chow, K.W.; Grimshaw, R.H.J.; Ding, E. *Wave Motion* **2005**, 43, 158-166.
[35] Slyunyaev, A.V. *Journal of Experimental and Theoretical Physics* **2001**, 92, 529-534.
[36] Lamb, K.G.; Polukhina, O.; Talipova, T.; Pelinovsky, E.; Xiao, W.; Kurkin, A. *Phy. Rev. E* **2007**, 75, 046306.

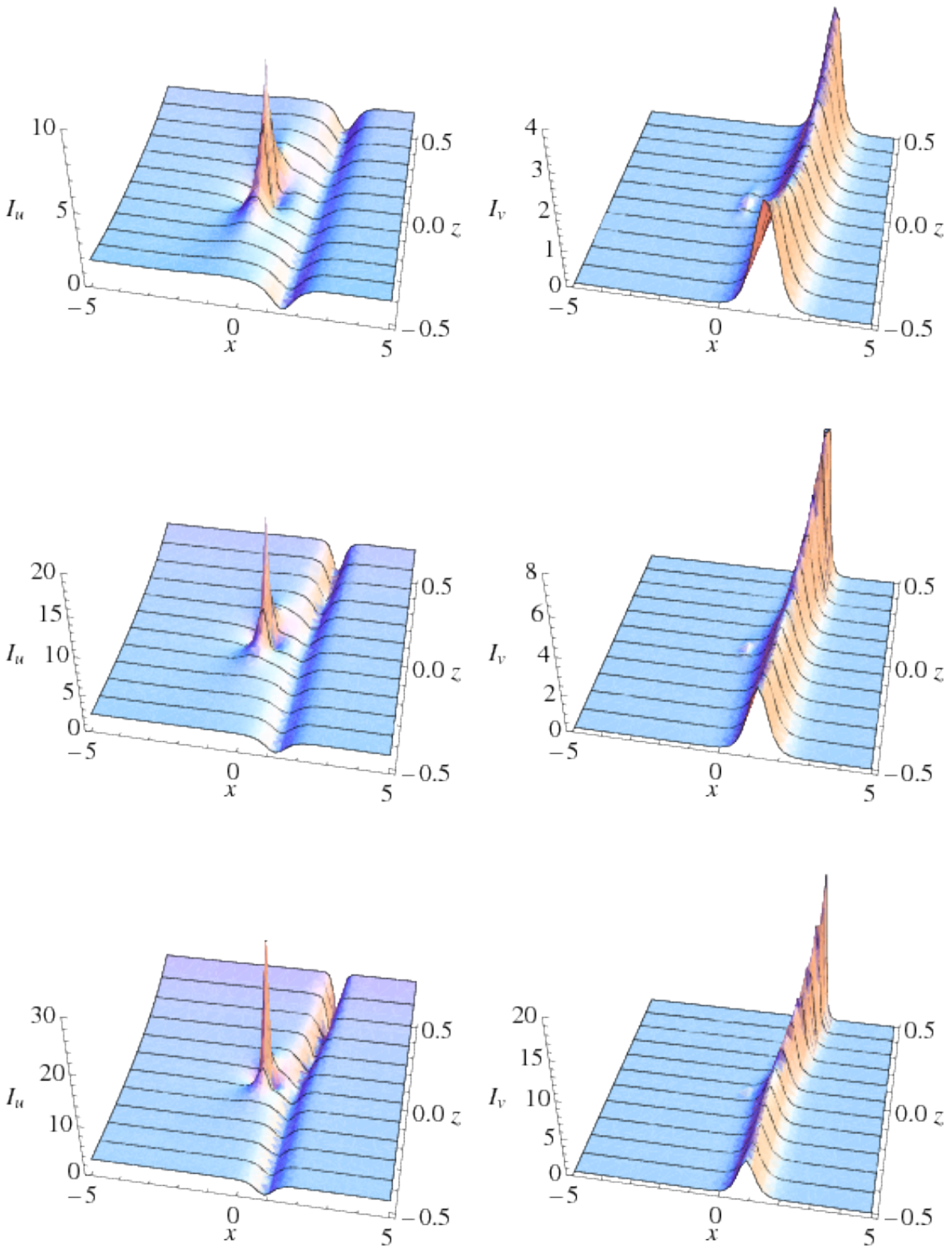

Figure 6. Freak wave intensity patterns for generalized tapering. The wave parameters are $a_1 = 1, a_2 = 0, h = 0.1$. Riccati parameter $c = 10, 1$, and 0.4 for plots at the top, middle and bottom.

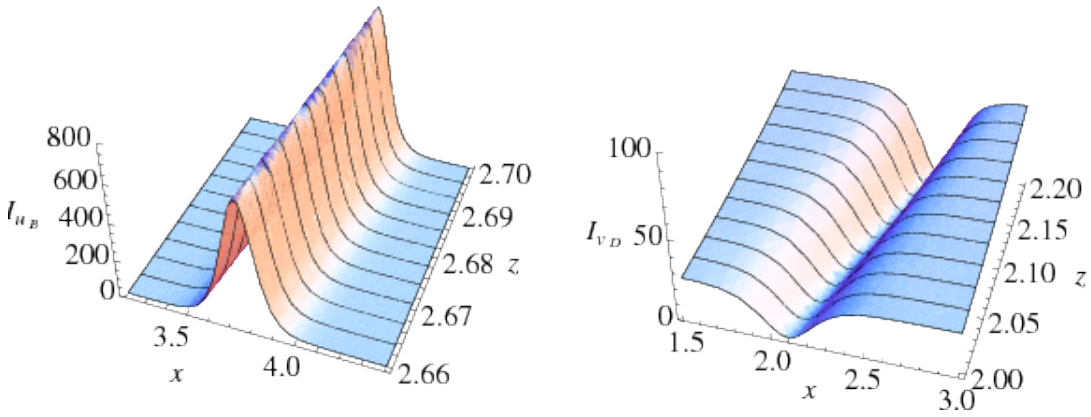

Figure 7. Intensity profiles of bright and dark solitons with $r_{11} = 5, r_{12} = 6, r_{21} = 6, r_{22} = 8$ and $p = .5$.

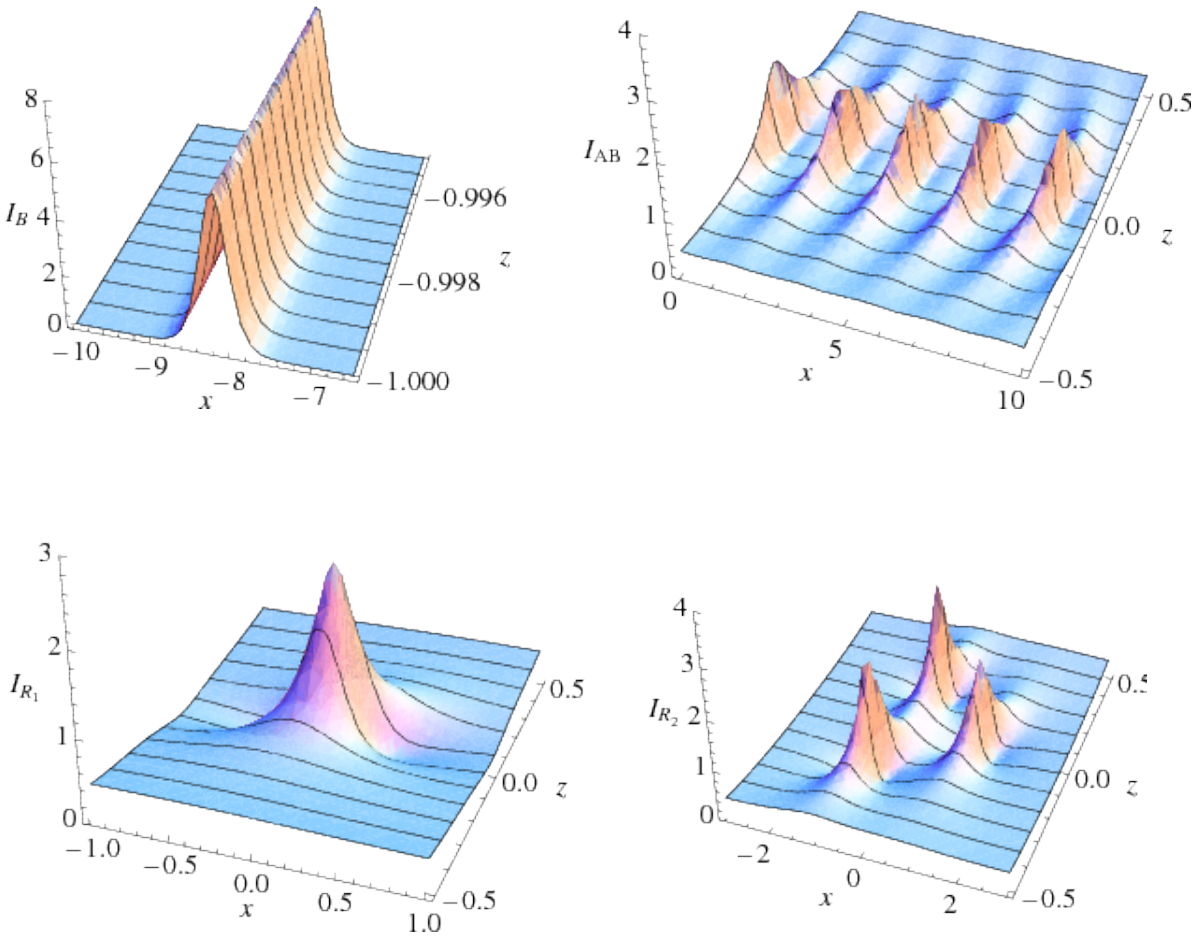

Figure 8. Intensity profiles of self-similar bright soliton, Akhmediev breather, first-order rogue wave and second-order rogue wave, respectively, with $r_{11} = 5, r_{12} = 6, r_{21} = 6, r_{22} = 8$ and $v = 2$.

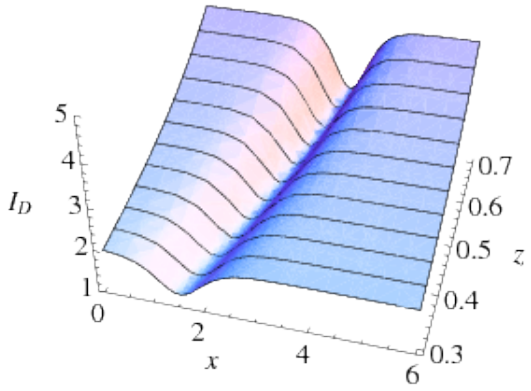

Figure 9. Intensity profile of self-similar dark soliton, with $v = 1$ and $q = 0.8$.